Direct Observation of Charge, Energy and H-transfer between the Backbone and Nucleobases in Isolated DNA Oligonucleotides

Min Liu,[a] David O'Reilly,[a] Lucas Schwob,[b] Xin Wang,[c] Vicente Zamudio-Bayer,[e] J. Tobias Lau,[e,f] Sadia Bari,[b] Thomas Schlathölter[c,d] and Jean-Christophe Poully*[a]

[a] Min Liu, David O'Reilly and Dr. Jean-Christophe Poully
CIMAP UMR 6252
CEA/CNRS/ENSICAEN/Université de Caen Normandie
Bd Becquerel 14070 Caen, France
E-mail: poully@ganil.fr
[b] Dr. Lucas Schwob, Prof. Dr. Sadia Bari
Deutsches Elektronen-Synchrotron DESY
22607 Hamburg, Germany
[c] Xin Wang, Dr. Thomas Schlathölter
Zernike Institute for Advanced Materials
University of Groningen
Groningen, The Netherlands
[d] Dr. Thomas Schlathölter,
University College Groningen
University of Groningen
Groningen, The Netherlands
[e] Prof. Dr. J. Tobias Lau
Physikalisches Institut
Albert-Ludwigs-Universität Freiburg
Freiburg, Germany
[f] Dr. V. Zamudio-Bayer, Prof. Dr. J. Tobias Lau
Abteilung für Hochempfindliche Röntgenspektroskopie
Helmholtz-Zentrum Berlin für Materialien und Energie
Berlin, Germany

Supporting information for this article is given via a link at the end of the document.

Abstract: Understanding how charge and energy as well as protons and hydrogen atoms are transferred in molecular systems as a result of an electronic excitation is fundamental for understanding the interaction between ionizing radiation and biological matter on the molecular level. In order to localize the excitation at the atomic scale, we have chosen to target phosphorus atoms in the backbone of gas-phase oligonucleotide anions and cations, by means of resonant photoabsorption at the L- and K-edges. The ionic photoproducts of the excitation process were studied by a combination of mass spectrometry and X-ray spectroscopy. The combination of absorption site selectivity and photoproduct sensitivity allowed the identification of X-ray spectral signatures of specific processes. Moreover, charge and/or energy as well as H transfer from the backbone to nucleobases has been directly observed. While the probability of one *vs.* two H transfer following valence ionization depends on the nucleobase, ionization of sugar or phosphate groups at the carbon K-edge or the phosphorus L-edge mainly leads to single H transfer to protonated adenine. Moreover, our results indicate a surprising proton transfer process to specifically form protonated guanine after excitation or ionization of P 2p electrons.

Introduction

The earliest stages of the action of ionizing radiation on biological systems comprise primary radiation-induced excitation and/or ionization processes, followed by a cascade of charge, energy and matter transport processes. In order to investigate these processes in detail, ideally the initial excitation/ionization event needs to be as localized as possible, which represents an experimental challenge at the molecular scale. In molecular collisions studies involving projectile ions or electrons, site selectivity would imply a reduction of the range of impact parameters to selectively ionize or excite a single atom or at least one chemical group. As this is technically impossible, much attention has been devoted to photoabsorption in the UV, VUV and X-ray ranges, where photon energy can be tuned to selectively target one atom or group in a molecular system and follow the relaxation dynamics. Gas-phase studies are particularly suitable to study VUV and soft X-ray induced processes in molecules, as they allow for investigating the genuine molecular response without any effects of a surrounding medium. Studying molecular ions rather than neutrals adds the possibility of manipulation by electric and magnetic fields, as well as molecular analysis thanks to mass spectrometry. In particular, target molecular ions can be selected for the irradiation, and the mass-over-charge (m/z) ratio of product ions can be obtained in order to reveal ionization, fragmentation and electron, proton or hydrogen transfer.

Regarding site-selective ejection of electrons from molecular systems in the gas phase, UV lasers have been used to induce electron photodetachment from deprotonated groups of oligonucleotides,[1] peptides and proteins,[2] but also lipids and polysaccharides.[3] Interestingly, it has been found that inducing backbone fragmentation of radicals formed by electron detachment to polymer molecules is valuable for their sequencing.[4] Photons in the VUV range have been used for

valence ionization of biomolecular ions,[5–8] however it is often difficult to localize the ionization event, due to the usually higher delocalization of the valence electrons compared to core electrons. To circumvent this, it is possible to use derivatized peptides with aromatic tags of ionization energy lower than any other group in the peptide, for instance allowing for ionization after absorption of a single photon of 7.9 eV thanks to a fluorine laser.[9] The resulting radical cation was found to be stabilized by charge delocalization over the backbone. To go further in precision, it is straightforward to target core electrons in atomic orbitals. Thanks to soft X-ray photoelectron spectroscopy in the gas phase and synchrotron radiation, pioneering studies have revealed the binding energy of 1s electrons of light atoms – for instance, carbon and oxygen atoms in small molecules such as CO_2 or H_2O, and described the Auger electron emission processes triggered by the creation of a 1s vacancy.[10] More recently, this technique was applied to neutral amino acids,[11,12] small peptides[13] as well as nucleobases,[14,15] which allowed demonstrating that the binding energy of 1s electrons is not strongly sensitive to neighboring atoms. However, more biologically-relevant systems such as peptides, proteins and DNA oligonucleotides have to be brought in the gas phase by soft techniques such as electrospray ionization (ESI) or matrix-assisted laser-induced desorption ionization, and accumulated in ion traps to reach sufficient molecular density and thus decent signal/noise ratio from photoabsorption through the detection of product ions formed by ionization and/or fragmentation processes. Therefore, since 2010, these systems have been investigated by near edge X-ray absorption fine structure action spectroscopy combined with mass spectrometry, and Auger electron emission as a consequence of excitation or ejection of 1s electrons from carbon, nitrogen or oxygen atoms has been shown to occur.[6,16,17] However, these atoms are distributed all over these molecules, complicating the task of linking a product ions to a given absorption site. For this reason, Schwob *et al*.[18] have chosen to study the methionine enkephalin peptide upon photoabsorption at the sulfur L-edge, since this molecule contains only one sulfur atom. They have demonstrated that specific photoabsorption leads to fragmentation near the excitation site. Very recently, specific photoabsorption at the K-edge of the fluorine atom located in the fluorouracil nucleobase of a trinucleotide has been carried out, surprisingly mostly leading to product ions from the two other nucleobases.[19] Such inverse effect has also been reported for the same oligonucleotide after ionization of nitrogen atoms.[20] However, the underlying mechanism is still unclear. In order to specifically target the DNA backbone, it is possible to tune the photon energy to target the phosphorus core electrons of 1s orbitals around 2150 eV: previous studies have reported specific fragmentation of a backbone P–O bond of a dinucleotide in the solid phase,[21] more efficient double-strand breaks in DNA plasmids,[22] and even chromosome aberrations in cells.[23]

Here, we study photoabsorption of isolated oligonucleotides around the phosphorus K- and L-edges. We analyze product anions and cations of single photon absorption by mass spectrometry, to demonstrate that specific absorption at phosphorus atoms triggers charge, energy and H transfer from backbone to nucleobases. Moreover, we investigate more deeply the H transfer processes within a protonated small oligonucleotide, and the role of the excited states reached after photoabsorption.

Results and Discussion

First, we demonstrate that specific photoabsorption at the backbone phosphorus atoms of an isolated deprotonated DNA oligonucleotide is achieved. We have chosen the oligonucleotide dCGCGGGCCCGCG, containing 11 phosphorus atoms and containing 50% guanine and 50% cytosine. Since guanine has the lowest ionization energy of all nucleobases, it is known to be a hole sink in nucleosides as well as oligonucleotides in the gas phase. Indeed, fragmentation of guanosine and thymidine following valence ionization mainly results in guanine and sugar-related fragment ions, respectively.[24] Regarding oligonucleotides, valence ionization induces fragmentation in G-rich regions, implying efficient hole transfer.[8] Therefore, dCGCGGGCCCGCG is a good candidate for backbone-base charge transfer.

Studying X-ray absorption around the phosphorus K-edge is challenging, because the absorption cross-section at this photon energy (around 2150 eV) is about 1.3 $x10^5$ Barn/atom, one order of magnitude lower than that of carbon around 300 eV (around 9.2$x10^5$ Barn/atom.[25] Moreover, oligonucleotides contain many more carbon than phosphorus atoms, for instance 114 against 11 in dCGCGGGCCCGCG. In order to compensate for the low cross section, X-ray exposure times had to be increased by one order of magnitude as compared to our previous study of deprotonated oligonucleotides at C K-edge.[26] From X-ray absorption studies on DNA in aqueous solution, it is known that the 2145 – 2185 eV energy range features a sharp resonance around 2152 eV (due to excitation of a 1s P electron into an unoccupied molecular orbital with overlapping P sp3 and O 2p atomic orbitals), and a much broader peak around 2165 – 2170 eV (assigned to photoelectron scattering on oxygen atoms of phosphate groups).[27] Importantly, an early previous work on isolated proteins has demonstrated that resonant features in K-shell X-ray spectra for the gas-phase are energetically very similar to the respective data from condensed-phase experiments.[16]

In this study, ionic products of $[dCGCGGGCCCGCG\text{-}4H]^{4-}$ and $[dCGCGGGCCCGCG\text{-}5H]^{5-}$ in the gas phase after single photon absorption following irradiation by synchrotron light were analyzed by time-of-flight mass spectrometry. Mass spectra of anionic and of cationic products were recorded for X-ray mean photon energies of 2143 eV (below K-edge), 2151 (on the resonance), 2163 and 2178 eV. The resolution of 8 eV FWHM provided by the beamline monochromator ensures that the peaks corresponding to those photon energies are separated. For both 4- and 5- charge states, the most abundant negative ion created by single-photon absorption is due to non-dissociative single electron detachment (NDSED) (see the mass spectra in Fig. S1 of the supporting information). The other peaks are due to scission of the DNA backbone and have much lower yields as compared to NDSED, especially taking into account the lower detection efficiency at higher *m/z* ratios. This very low fragmentation yield is due to the large size of the system: we have observed such a phenomenon after VUV and X-ray photoabsorption of deprotonated oligonucleotides as well as protonated peptides and proteins.[8,26,28,29] In Fig. 1, we show the relative yield of NDSED from $[dCGCGGGCCCGCG\text{-}4H]^{4-}$ after single-photon absorption (see Fig. S2 for $[dCGCGGGCCCGCG\text{-}5H]^{5-}$). Around the carbon K-edge, this yield slightly decreases from 288 to 300 eV, consistent with the

transition from single to multiple ionization observed in this range for protonated peptides and proteins.[16,30] Strikingly, from 2143 (below the phosphorus K-edge) to 2151 eV (on the resonance), the relative yield of NDSED increases by over a factor of two. Below the edge, mainly multiple electron ejection is expected from the valence shell or from 1s orbitals of C, N and O atoms, since 2143 eV is far higher than their corresponding ionization energies. In contrast, at the phosphorus K-edge resonance energy, photoabsorption by phosphorus atoms is expected to trigger excitation of one P 1s electron to an unoccupied P=O molecular orbital,[31] followed by emission of one high-energy Auger electron, resulting in more single electron detachment compared to 2143 eV. From 2151 to 2163 eV, the yield of NDSED from dCGCGGGCCCGCG stays roughly constant (*cf.* Fig. 1 and S2), but it decreases at 2178 eV, consistent with the transition from excitation to ejection of 1s electrons, leading to more multiple- and thus less single-electron detachment. The same conclusions can be made for $[dCGCGGGCCCGCG\text{-}5H]^{5-}$ from the data appearing in Fig. S2 (see the SI). Since this behavior has also been observed at the C, N and O K-edges of proteins[16] as well as the C K-edge of deprotonated DNA oligonucleotides,[26] it supports our present attribution of specific photoabsorption at the backbone phosphorus atoms of the studied oligonucleotide.

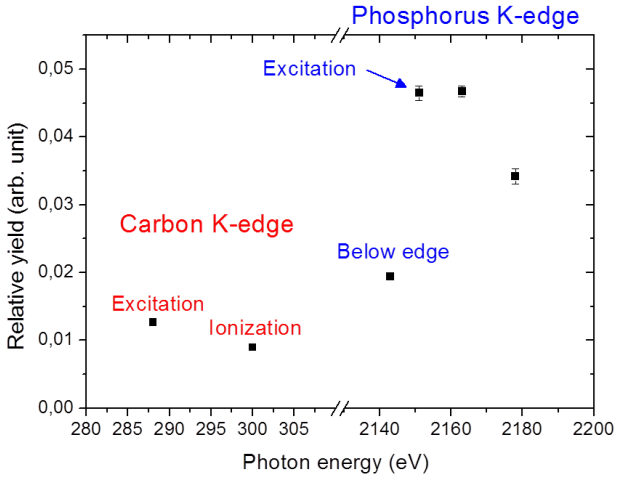

Figure 1. Relative yield of non-dissociative single electron detachment from $[dCGCGGGCCCGCG\text{-}4H]^{4-}$ after single photon absorption, as a function of photon energy, obtained by calculating the area under the peak in the mass spectrum and normalizing by the area under the precursor depletion peak. Error bars represent the standard deviation of the average value from three independent calculations (n = 3). The energy regions corresponding to carbon and phosphorus K-edges are indicated in red and blue, respectively.

Now, we will show in the next two paragraphs that charge and/or energy as well as H/H^+ are transferred from backbone to nucleobases within the dCGCGGGCCCGCG oligonucleotide after photoabsorption. In the previous paragraph, we have seen that NDSED is the main process responsible for the formation of negative ions from $[dCGCGGGCCCGCG\text{-}4H]^{4-}$ and $[dCGCGGGCCCGCG\text{-}5H]^{5-}$ following photoabsorption around the C and P K-edges. However, the NDSED relative yield is low, as it appears to be much more probable that the decay of an initial 1s vacancy involves detachment of several valence electrons. This process is followed by extensive fragmentation, as very recently demonstrated for deprotonated oligonucleotides.[26] Consistently, in the present case, we detected abundant small fragment cations from deprotonated $[dCGCGGGCCCGCG\text{-}nH]^{n-}$ after photoabsorption around the C and P K-edges (see mass spectra in Fig. 2 for the 4- charge state, very similar spectra were observed for the 5- charge state at the P K-edge). In these mass spectra, the most intense peaks can be assigned to the same singly-charged fragments as for other deprotonated oligonucleotides. The lightest ones are the guanine radical cation and protonated guanine (*m/z* = 151 and 152, respectively) as well as loss of NH_3 from the latter. Cytosine-related ions are not observed because their *m/z* ratios (around 110) are below the low-mass cutoff of the Paul ion trap. The peaks at *m/z* = 232 and 192 are due to fragments containing the guanine or cytosine nucleobase, respectively, and one sugar ring (see Scheme 1): they have been observed after collision-induced dissociation (CID) and ionization of multiply-protonated oligonucleotides,[6,32] and assigned to cyclic nucleosides, they are thus noted cG^+ and cC^+. The peak at *m/z* = 301 has previously been assigned to the guanine dimer formed after cleavage of two glycosidic bonds and one H or proton transfer, but another fragment might also explain the presence of this peak: it is noted Gua^+, and includes part of a neutral phosphoric acid group as well as one guanosine moiety (see Scheme 1): this fragment requires the transfer of two H atoms or one H and one proton. Note that the fragments at *m/z* = 232 and 192 require the cleavage of backbone bonds (see Scheme 1) that have been shown to be also broken in the case of irradiation of DNA in solution by UV or protons at 70 MeV kinetic energy.[27] Nucleobase-related ions are formed after cleavage of the glycosidic bonds linking the backbone to nucleobases. Interestingly, the two peaks assigned to the fragments noted $Back_1^+$ and $Back_2^+$ are more intense for dCGCGGGCCCGCG than for previously studied oligonucleotides: they both contain a sugar moiety and a phosphate group (minus OH for $Back_2^+$), and are therefore due to cleavage of two backbone bonds and one glycosidic bond (*cf.* Scheme 1). The mass spectrum at 2143 eV photon energy is very similar to the ones at the C K-edge energies of 288 and 300 eV (data not shown). Strikingly, $Back_1^+$ becomes much more abundant at the P K-edge excitation energy of 2151 eV (*cf.* Fig. 2). This increase indicates localized fragmentation after site-specific photoabsorption at the phosphorus atoms and thus at the oligonucleotide's backbone. In addition, a surprising increase of the relative abundance of guanine-related ions is also observed at 2151 eV and above. In the next paragraph, we discuss this result more deeply.

Since phosphate groups are the most acidic sites in oligonucleotides, nucleobases are not expected to carry a negative charge in deprotonated oligonucleotides, if the oligonucleotide's charge state is lower than the number of phosphate groups (which is the case here), as found by CID experiments.[33] Therefore, nucleobases are most probably initially neutral in $[dCGCGGGCCCGCG\text{-}4H]^{4-}$ and $[dCGCGGGCCCGCG\text{-}5H]^{5-}$: thus, to account for the observation of G-related cations (see Fig. 2), guanine has to become positively charged after photoabsorption at P atoms. We see three possible mechanisms: the first is ionization of the backbone followed by hole transfer to the base, the second is electronic excitation of the backbone and transfer of this excitation energy to a base followed by ionization of this base, and the third is proton transfer to the base. The initial electronic

and geometrical structures of deprotonated oligonucleotides are valuable for discussing these mechanisms. Daly *et al.*[1] studied multiply-deprotonated dG_6, dA_6, dC_6 and dT_6 oligonucleotides by means of quantum-chemical calculations, ion-mobility spectrometry, IRMPD and UV spectroscopy, and found that charge state has a major effect on their geometrical structure: 4- oligonucleotides are unfolded because of Coulomb repulsion, while lower charge states are more compact. The same trend has been observed for deprotonated dT_{10} from 3- to 6- charge states by Hoaglung *et al.*[34] Therefore, we can expect partially unfolded conformers to be present in our experiments. In particular, we expect the three central guanines in dCGCGGGCCCGCG to be stacked, like in $[dG_6\text{-}3H]^{3-}$, which would stabilize the hole after transfer from the backbone (*cf.* mechanism 1). Indeed, holes located in valence orbitals are likely to be transferred to guanine-rich regions,[8] which would then lead to guanine-related cations after glycosidic bond cleavage. In mechanism 2, the ejected electron might come from the valence shell located in the guanine-rich region, since in the case of $[dG_6\text{-}3H]^{3-}$, Daly *et al.*[1] have found by quantum-chemical calculations that the electron density of molecular orbitals close to the HOMO in energy is high in the five stacked guanines. Mechanism 3 (proton transfer to the base) seems less probable given the partially unfolded geometrical structure of the oligonucleotides that disfavor the formation of H bonds. The conclusion of this paragraph is that our present results unambiguously demonstrate transfer of charge and/or energy from backbone to nucleobases after photoabsorption and ionization.

Formation of protonated nucleobases is a common process after ionization of neutral nucleosides,[24,35] but also after ionization of protonated or deprotonated oligonucleotides,[6,26] for a variety of ionizing particles. It is interesting to notice that this process requires the transfer of two H atoms or of one H and one proton in addition to cleavage of one of the glycosidic bonds linking nucleobase and sugar moieties. For instance, here, to create protonated guanine, glycosidic bond cleavage is typically followed by H-transfer to form either neutral guanine or its radical cation, and a subsequent proton or H transfer is needed. Although transfer from another nucleobase is in principle possible, it is not supported by the observation of protonated nucleobases after ionization of sugar groups in neutral nucleosides, which only contain one nucleobase.[24,35] In the following, we investigate more thoroughly these H/H^+ transfer processes induced by specific photoabsorption at the DNA backbone.

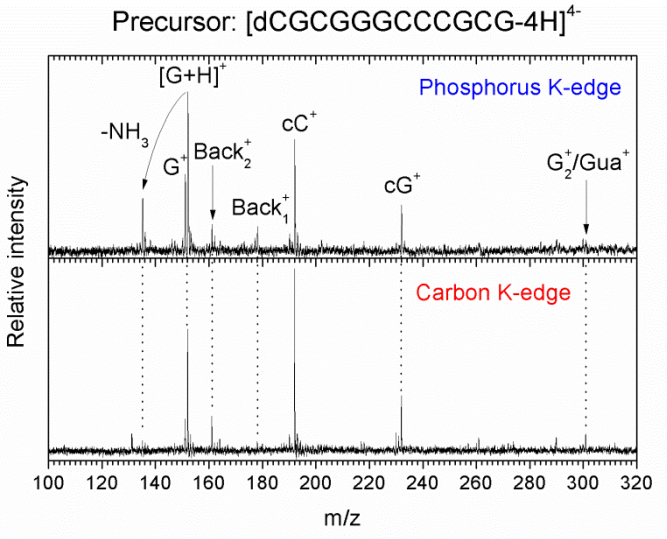

Figure 2. Mass spectra of positive ions formed from $[dCGCGGGCCCGCG\text{-}4H]^{4-}$ after single photon absorption around carbon and phosphorus K-edges (photon energy 300 and 2151 eV, respectively). Guanine radical cation and protonated guanine are denoted G^+ and $[G+H]^+$, respectively. cC^+ and cG^+ correspond to cyclic cytidine and guanosine nucleosides, $Back_1^+$ and $Back_2^+$ to backbone fragments, G_2^+ to the guanine dimer and Gua^+ to a fragment shown in Scheme 1.

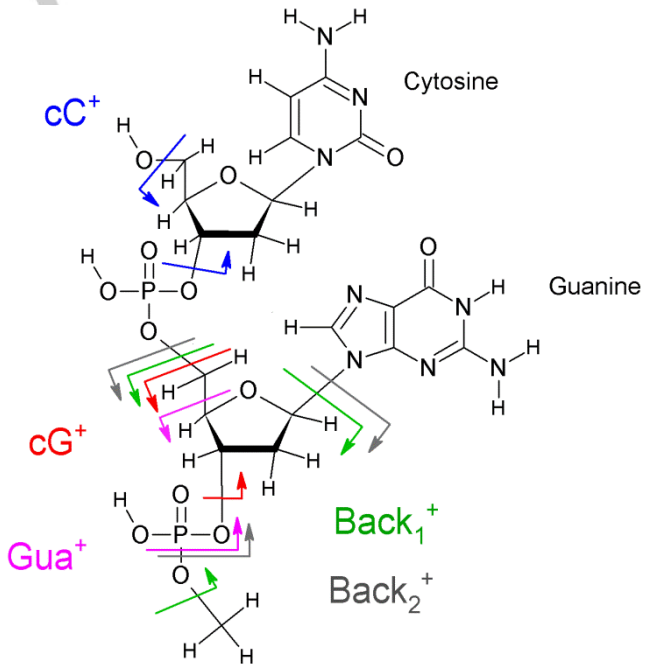

Scheme 1. Chemical structure of the two first nucleotides of the dCGCGGGCCCGCG oligonucleotide. The bonds that need to be cleaved to form the $Back_1^+$, $Back_2^+$, cG+, cC+ as well as Gua^+ fragments are spotted with green, red, blue and purple lines with arrows indicating on which side of the bond the positive charge is located.

Very recently, H/H^+ transfer processes within the $[d^FUAG+H]^+$ protonated oligonucleotide (^FU being the halogenated nucleobase fluorouracil) after photoabsorption at C, N, O and F K-edges have been investigated in great detail.[19] It was found that these processes occur with a high probability, irrespective of the photoabsorbing site in the oligonucleotide (backbone or nucleobase). However, photoabsorption at the backbone could

only be deduced thanks to comparison between the experimental data and quantum chemical calculations: here, we use the same experimental approach but we directly target the backbone P atoms by choosing a photon energy range around their L-edge (140 eV). Product cations of photoabsorption are then analyzed by mass spectrometry. The same peaks as previously reported[19,20] have been observed in the mass spectra (*cf.* Fig. S3): they are mainly due to cleavage of the glycosidic bonds together with H and/or proton transfer and formation of nucleobase-related ions, either radical cations or protonated. The yield of each of these fragment ions as a function of photon energy is visible in Fig. 3. The global trend is the same for all ions: a smooth decrease when photon energy rises, with superimposed structures around 140 and 147 eV. This decrease is due to non-resonant ejection of electrons located in molecular valence orbitals, whose cross-section follows a power law according to previous studies.[19] The superimposed structures are assigned to specific photoabsorption by phosphorus atoms at the L-edge, following the studies of Kruse *et al*.[36] on powders of nucleotides and RNA, as well as those of Neville *et al*.[37] on OPF_3 in the gas phase.

In the following, we will focus on the relative abundance of nucleobase-related fragments from Fig. 3, without considering the peaks due to specific photoabsorption at the P L-edge, which means discussing only valence photoionization. We can see that in the whole photon energy range, fluorouracil ions are the least abundant nucleobase fragments, which is consistent with previous studies that attributed this fact to the high ionization energy of fluorouracil compared to adenine (A) and guanine (G).[20] The underlying process is hole transfer after valence ionization: we have previously studied it for other deprotonated oligonucleotides as well as neutral nucleosides.[8,24] However, ionization energy is not the only parameter governing the relative amount of nucleobase cations, since it is 8.6 ± 0.3 eV for adenine against 8.0 ± 0.2 eV for guanine,[38] but $[A+H]^+$ is more abundant than guanine cations in Fig. 3. The reason is probably the initial protonation of adenine in $[d^FUAG+H]^+$,[20] which allows for the formation of adenine cations without charge transfer: only H transfer to adenine and glycosidic bond cleavage is required for releasing $[A+H]^+$. Its high abundance might be linked to a low potential energy barrier for H transfer, but we will see that the stability of products probably plays a more important role here. The second more abundant nucleobase-related ion is $[G+H]^+$, which needs the transfer of two H atoms (if guanine has one positive charge as a result of photoabsorption) or one H and one proton. Since guanine has the lowest ionization energy among the DNA and RNA nucleobases, it is the most probable site where the hole created by valence photoionization ends: therefore, it is likely that two H atoms are transferred to positively-charged guanine, before or after glycosidic bond cleavage. From the lower amount of guanine radical cation, we can infer that transfer of one H is less likely, which might seem surprising. However, if one considers that protonated molecules as end-products are usually more stable than radical cations, this behavior may be explained by a reaction in the ground-state potential energy surface of the ionized species, with a sufficiently high amount of vibrational energy to overcome all barriers needed for several H transfers and glycosidic bond cleavage. In protonated peptides and proteins, this vibrational energy has been estimated to be around 20 eV after photoabsorption at the carbon K-edge (around 300 eV photon energy).[29] It is most probably similar at the phosphorus L-edge, since almost the same mass spectra have been observed for $[d^FUAG+H]^+$. 20 eV is much higher than calculated or measured barriers for glycosidic bond cleavage or H transfer after ionization of isolated biomolecules, therefore supporting our hypothesis.[39–42]

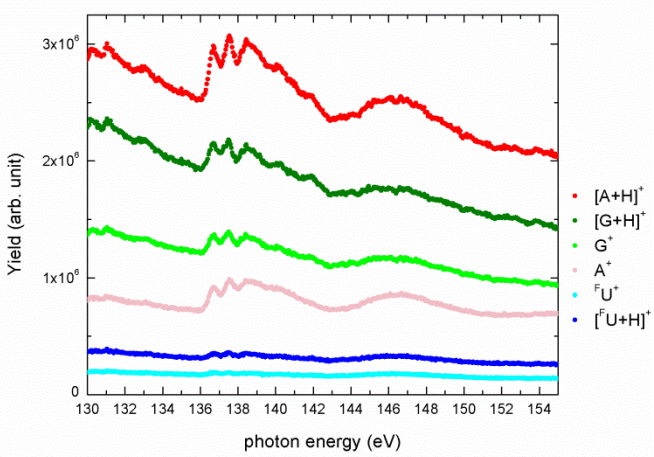

Figure 3. Yield of positive ions formed from $[d^FUAG+H]^+$ after single photon absorption around the phosphorus L-edge, as a function of photon energy. Nucleobase radical cations and protonated nucleobases are denoted B^+ and $[B+H]^+$, respectively, replacing B by A for adenine, G for guanine or ^FU for fluorouracil.

Now, let us discuss the yield of the nucleobase-related ions created after specific photoabsorption at the phosphorus L-edge and thus at the oligonucleotide backbone phosphate groups. To extract this relative abundance, we have subtracted the yield of photocations formed by valence ionization from the total yield shown in Fig. 3. This subtracted yield was estimated by fitting a function of the form $y = AE^{-p}$ (A and p being adjustable parameters) to the pre-edge data (130 – 136 eV) for each cation appearing in Fig. 3. The results are shown in Fig. 4: for all cations, the obtained yield is close to zero at low photon energy, rises sharply around 136.2 eV and shows two main peaks around 139 and 147 eV. The overall trend of the spectra is similar to those of powders of nucleotides and RNA[36] as well as isolated OPF_3.[37] The obtained spectra for $[A+H]^+$ and $[G+H]^+$ are shown in Fig. 4 (bottom), where one can clearly see the fine structure of the peak around 139 eV. Resonances are observed at 136.7, 137.5, 138.7, 140.3 and 141.9 eV for all fragment cations. The first three resonances are close to those reported for powders of nucleotides and RNA[36] (136.1, 137.1 and 138.5 – 138.9 eV) as well as isolated OPF_3 (137.1, 137.8 and 138.9 eV),[37] we can thus assign them to excitation of $2p_{1/2}$ or $2p_{3/2}$ electrons of phosphorus to unoccupied 3s-like and 3p-like antibonding orbitals, the latter being mixed with O character. The resonances at 140.3 and 141.9 eV are not resolved in the case of powders of nucleotides and RNA, we thus only have the study on OPF_3 as a reference: an intense resonance assigned to excitation of 2p electrons to P 4s Rydberg states has been observed at 140.4 eV, and a weaker feature around 142.5 eV involving excitation to P 3d orbitals. The large feature centered around 147 eV is assigned to excitation of 2p electrons to O=P π* antibonding orbitals with a large contribution of the 3d orbitals of phosphorus, since a similar feature is detected at 148 eV for OPF_3.[37] and 146.5-147 eV for powders of nucleotides and

RNA.[36] Overall, these results show that the energy position of these resonances involving excitation of 2p electrons of phosphorus is not heavily affected by molecular environment, *e. g.* when going from the gas to the condensed phase, and from OPF_3 to an oligonucleotide. It is also important to note that direct ionization due to ejection of one 2p electron to the continuum has been reported to start around 143-144 eV for OPF_3,[43] with a cross-section smoothly increasing to dominate only for photon energies around 160 eV, higher than the present experimental range.

Interestingly, after specific photoabsorption at the L-edge of phosphorus atoms of $[d^FUAG+H]^+$, the relative abundance of nucleobases changes compared to the case of valence ionization (see Fig. 3 and 4): more adenine- than guanine-related ions are produced. A very similar behavior has been observed at the carbon K-edge, for photon energies corresponding to excitation of backbone carbon atoms according to quantum-chemical calculations.[19] Backbone carbons are only present in sugar groups, which indicates that ionization of sugar groups favors the formation of adenine-related ions in $[d^FUAG+H]^+$. Among these ions, protonated adenine dominates, whose formation requires single H transfer most probably from sugar groups as discussed above. This indicates that single H transfer occurs from sugar groups after their ionization. Besides, previous investigation of the geometrical structure of $[d^FUAG+H]^+$ in its electronic ground state was carried out by means of quantum-chemical calculations,[19,20] and one H-bond was found between a CH_2 belonging to the sugar group linked to protonated adenine and one of its nitrogen atoms: it was thus assumed that H transfer proceeds through this H-bond. In the present case of photoabsorption at the phosphorus L-edge, electronic excitation at a phosphoric acid group occurs, and our results show that efficient H transfer to protonated adenine also follows.

Another interesting observation can be made by comparing the relative intensity of the bands around 140 and 147 eV, the latter being much higher for fluorouracil cations compared to adenine and guanine. Since we assigned these bands to different electronic excited states within the phosphoric acid group, we conclude that the formation of nucleobase cations is influenced by these excited states. It is in contrast with the usual behavior of molecular systems after ionization and electronic excitation: fragmentation in the electronic ground-state after internal conversion.[29,44] Another evidence of the role of excited states in the formation of protonated adenine and protonated guanine can be found in Fig. 5, where the ratio of their yield over the yield of radical cations is plotted *vs.* photon energy (the statistics is too poor for fluorouracil). Indeed, for guanine, a peak is seen around 142.5 eV: it is very close to the energy of the peak observed in Fig. 4 and assigned to excitation of P 2p electrons to P 3d orbitals. Such selective enhancement of the production of protonated guanine *vs.* radical cation might be explained by excited-state proton transfer, since this process plays an important role in molecular systems in general and DNA in particular.[45] In the S_1 state of isolated neutral guanosine, quantum-chemical calculations have predicted a potential energy barrier lower than 0.7 eV for proton transfer from the sugar moiety to guanine through an H bond.[46] Direct measurement of excited-state dynamics has been carried out for nucleosides after VUV photoionization *via* a pump-probe approach:[47] such experiments would be highly valuable for confirming our results on oligonucleotides. We also observe in Fig. 5 an increase of the $[G+H]^+/G^+$ ratio from 148 eV: this might be due to the onset of ionization of P 2p electrons in $[d^FUAG+H]^+$, which would trigger proton transfer from the backbone to guanine. Ionization-induced proton transfer is well known in molecular systems (especially DNA building blocks) in the gas phase, and has been shown to occur with very low or even no barrier in the electronic ground state.[24,48–55] The fact that the $[A+H]^+/A^+$ ratio is much less affected by photon energy and in average higher than the $[G+H]^+/G^+$ ratio is probably explained by the initial protonation of adenine in $[d^FUAG+H]^+$.

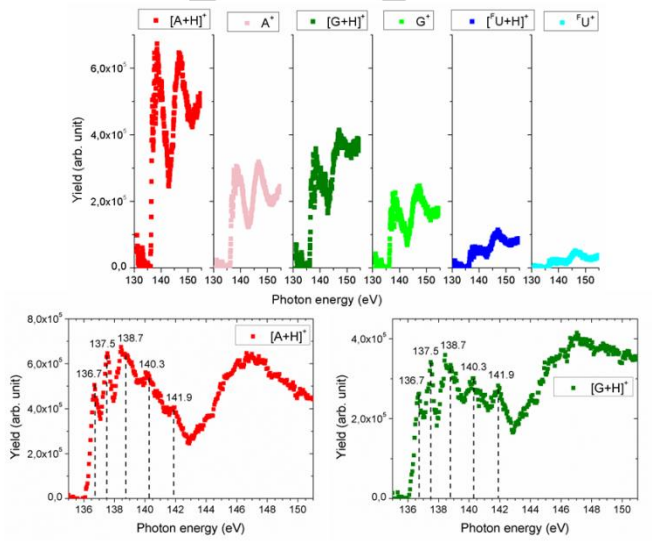

Figure 4. Yield of positive ions formed from $[d^FUAG+H]^+$ after single photon absorption around the phosphorus L-edge, after subtraction of the background due to valence ionization (see the text), as a function of photon energy. Nucleobase radical cations and protonated nucleobases are denoted B^+ and $[B+H]^+$, respectively, replacing B by A, G or ^FU.

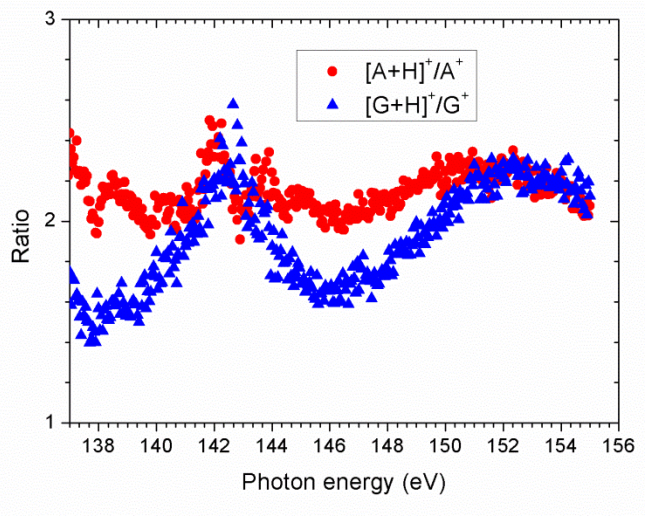

Figure 5. Ratio of the yields of protonated *vs.* radical cations of adenine (A) and guanine (G) nucleobases formed from $[d^FUAG+H]^+$ after single photon absorption around the phosphorus L-edge, after subtraction of the background due to valence ionization (see the text), as a function of photon energy. Nucleobase radical cations and protonated nucleobases are denoted B^+ and $[B+H]^+$, respectively, replacing B by A or G.

Conclusion

This contribution aims at exploring the consequences of specific photoabsorption at the backbone of DNA oligonucleotides in the gas phase, in terms of charge, energy as well as H transfer. By means of synchrotron radiation, we target phosphorus atoms in the backbone of isolated oligonucleotides by tuning the X-ray photon energy to their K- and L-edges (around 2160 and 140 eV, respectively), and we analyze the product ions by mass spectrometry. We report X-ray spectral signatures of specific photoabsorption, and unambiguously demonstrate that charge, energy as well as H transfer from the backbone to nucleobases occurs. Moreover, while the probability of one *vs.* two H transfer following valence ionization depends on the nucleobase, ionization of sugar or phosphate groups at the carbon K-edge or the phosphorus L-edge mainly leads to single H transfer to protonated adenine. We have also found evidence for a proton transfer process to specifically form protonated guanine after excitation or ionization of phosphorus 2p electrons.

Forthcoming investigations, especially experiments at XFEL facilities, should unravel the timescale for these transfer processes. Moreover, we plan to extend these studies to typical noncovalent DNA structures such as G-quadruplexes as well as double helices, for instance to know if and how charge, energy and H is transferred from one strand to another.

Experimental Section

Two types of experiments were carried out to study photoabsorption-induced processes in isolated DNA.

In the first type of experiments, a home-built tandem mass spectrometer was used. It has already been described in detail before.[29,56] For irradiating $[d(^{F}UAG)+H]^{+}$, it has been interfaced with the U49/2-PGM1 beamline at the BESSY II synchrotron (Berlin, Germany), with the same experimental parameters as previously reported, apart from photon energy.[19] For irradiating the deprotonated dCGCGGGCCCGCG oligonucleotide, the mass spectrometer was interfaced with the variable polarization XUV beamline P04[57] at the PETRA III synchrotron (Hamburg, Germany). The monochromator exit slit width was 500 and 1500 µm for photon energies around the carbon and phosphorus K-edges, respectively, corresponding to resolutions of 0.5 and 8 eV FWHM. We calibrated the beamline for photon energy in the 1700 – 2500 eV range with an electron spectrometer, by measuring the signal coming from photoexcitation of SF_6 around the sulfur K-edge (2486 eV[58]) followed by Auger decay, as well as photoionization threshold of electrons in 2p orbitals of krypton (1729 eV[59]). We assumed a linear shift between the real and beamline values of photon energy in this range. A solution of the dCGCGGGCCCGCG oligonucleotide (reverse-phase HPLC purity, Eurogentec, Seraing, Belgium) at 100 µM was made with 75% HPLC methanol, 25% deionized water and 5% ammonium hydroxide. The oligonucleotide solution was then sprayed by an in-house-built electrospray ionization (ESI) source under atmospheric conditions, using a syringe pump with a flow rate of about 0.15 mL/h. Thanks to a heated metallic capillary, the deprotonated oligonucleotide ions were then guided into a first vacuum chamber where a radio frequency (RF) ion funnel locates in. After phase space compression in the funnel, the ion beam was guided in an octopole RF ion guide. Subsequently, the precursor ion of interest was selected according to its mass-over-charge ratio in a quadrupole mass filter. This selected ion was then accumulated in a three-dimensional RF ion Paul trap to get sufficient target density. In the trap, a helium buffer gas pulse was used to thermalize the precursor ions by collisions. After accumulation, the photon beam went through the center of the trap to interact with the precursors. The interaction time was adjusted between 1000 and 4750 ms to ensure that less than 10% of the precursor ions underwent photoabsorption. In this case, single photon absorption dominates. After irradiation, the product ions were extracted into a reflectron time-of-flight (TOF) mass spectrometer and detected by a microchannel plate (MCP) detector. Either the negatively-charged products and precursors or the positively-charged products could be detected by switching the polarity of all voltages from the trap end caps to the detector. Mass spectra were recorded at the carbon K-edge and phosphorus K-edge energies.

The second type of experiments on a protonated oligonucleotide was carried out with the Ion Trap fixed end-station[60] at the high-resolution soft X-ray beamline UE52-PGM at the BESSY II synchrotron (Berlin, Germany). A solution of the $d^{F}UAG$ oligonucleotide (LGC Biosearch Technologies) at 20 µM was made with HPLC methanol with 2% acetic acid. The oligonucleotide cations were brought in the gas phase with an ESI source. After selection by a quadruple mass filter, the singly protonated $[d(^{F}UAG)+H]^{+}$ ions were guided to a cryogenic ($T \approx 20$ K) linear RF trap and stored there to measure the soft X-ray photoabsorption action spectra of $[d(^{F}UAG)+H]^{+}$ at the phosphorus L-edge. The photon energy was ramped in 0.05 eV step across the phosphorus L-edge (130 – 155 eV), and the trapped oligonucleotides were exposed to monochromatic ($\Delta E \approx$ 100 meV) soft X-rays at each photon energy. After interaction, the trap content was extracted into a reflectron TOF mass spectrometer and detected by MCPs for partial ion yield spectroscopy. From the obtained mass spectra, we plot the ion yield of the different photofragments as a function of photon energy, after normalization by photon flux.

Acknowledgements

We acknowledge DESY (Hamburg, Germany), a member of the Helmholtz Association HGF, for the provision of experimental facilities. Parts of this research were carried out at PETRA III and we would like to thank Moritz Hoesch and Florian Trinter for assistance in using the P04 beamline. Beamtime was allocated for proposal I-20210702 EC. We also thank HZB for granting us beamtime at BESSY II beamline UE52-PGM Ion Trap.

Keywords: oligonucleotides • charge transfer • photoabsorption • mass spectrometry • phosphorus

[1] S. Daly, M. Porrini, F. Rosu, V. Gabelica, *Faraday Discuss.* **2019**, *217*, 361–382.

[2] R. Antoine, P. Dugourd, *Phys. Chem. Chem. Phys.* **2011**, *13*, 16494–16509.

[3] C. Crittenden, E. Escobar, P. Williams, J. Sanders, J. Brodbelt, *Anal. Chem.* **2019**, *91*, 4672–4679.

[4] R. Antoine, J. Lemoine, P. Dugourd, *Mass Spectrom. Rev.* **2013**, *33*, 501.

[5] A. Giuliani, A. R. Milosavljevic, F. Canon, L. Nahon, *Mass Spectrom. Rev.* **2014**, *33*, 424–441.

[6] O. Gonzalez-Magana, M. Tiemens, G. Reitsma, L. Boschman, M. Door, S. Bari, P. O. Lahaie, J. R. Wagner, M. A. Huels, R. Hoekstra, T. Schlatholter, *Phys. Rev. A* **2013**, *87*, 032702.

[7] C. Brunet, R. Antoine, P. Dugourd, F. Canon, A. Giuliani, L. Nahon, *J. Chem. Phys.* **2013**, *138*, 064301.

[8] W. Li, E. Mjekiqi, W. Douma, X. Wang, O. Kavatsyuk, R. Hoekstra, J.-C. Poully, T. Schlathölter, *Chem. – Eur. J.* **2019**, *25*, 16114–16119.

[9] P. Edirisinghe, J. Moore, W. Calaway, I. Veryovkin, M. Pellin, L. Hanley, *Anal. Chem.* **2006**, *78*, 5876–5883.

[10] K. Ueda, *J. Phys. B-At. Mol. Opt. Phys.* **2003**, *36*, R1–R47.

[11] O. Plekan, V. Feyer, R. Richter, M. Coreno, M. de Simone, K. C. Prince, V. Carravetta, *J. Phys. Chem. A* **2007**, *111*, 10998–11005.

[12] H. Farrokhpour, F. Fathi, A. Naves De Brito, *J. Phys. Chem. A* **2012**, *116*, 7004–7015.

[13] A. Arachchilage, F. Wang, V. Feyer, O. Plekan, K. Prince, *J. Chem. Phys.* **2012**, *136*, DOI 10.1063/1.3693763.

[14] O. Plekan, V. Feyer, R. Richter, M. Coreno, M. de Simone, K. C. Prince, A. B. Trofimov, E. V. Gromov, I. L. Zaytseva, J. Schirmer, *Chem. Phys.* **2008**, *347*, 360.

[15] A. B. Trofimov, J. Schirmer, V. B. Kobychev, A. W. Potts, D. M. P. Holland, L. Karlsson, *J. Phys. B-At. Mol. Opt. Phys.* **2006**, *39*, 305–329.

[16] A. R. Milosavljevic, F. Canon, C. Nicolas, C. Miron, L. Nahon, A. Giuliani, *J. Phys. Chem. Lett.* **2012**, *3*, 1191–1196.

[17] S. Bari, D. Egorov, T. L. C. Jansen, R. Boll, R. Hoekstra, S. Techert, V. Zamudio-Bayer, C. Bülow, R. Lindblad, G. Leistner, A. Ławicki, K. Hirsch, P. S. Miedema, B. von Issendorff, J. T. Lau, T. Schlathölter, *Chem. – Eur. J.* **2018**, *24*, 7631–7636.

[18] L. Schwob, S. Dörner, K. Atak, K. Schubert, M. Timm, C. Bülow, V. Zamudio-Bayer, B. von Issendorff, J. T. Lau, S. Techert, S. Bari, *J. Phys. Chem. Lett.* **2020**, *11*, 1215–1221.

[19] X. Wang, S. Rathnachalam, V. Zamudio-Bayer, K. Bijlsma, W. Li, R. Hoekstra, M. Kubin, M. Timm, B. von Issendorff, J. T. Lau, S. Faraji, T. Schlathölter, *Phys. Chem. Chem. Phys.* **2022**, *24*, 7815–7825.

[20] X. Wang, S. Rathnachalam, K. Bijlsma, W. Li, R. Hoekstra, M. Kubin, M. Timm, B. von Issendorff, V. Zamudio-Bayer, J. T. Lau, S. Faraji, T. Schlathölter, *Phys. Chem. Chem. Phys.* **2021**, *23*, 11900–11906.

[21] H. Frohlich, M. LeMaire, F. Guillot, M. Tronc, J. Cosset, C. LeSech, *Nucl. Instrum. METHODS Phys. Res. Sect. B-BEAM Interact. Mater. At.* **1995**, *105*, 314–317.

[22] K. Hieda, T. Hirono, A. Azami, M. Suzuki, Y. Furusawa, H. Maezawa, N. Usami, A. Yokoya, K. Kobayashi, *Int. J. Radiat. Biol.* **1996**, *70*, 437–445.

[23] S. SAIGUSA, Y. EJIMA, K. KOBAYASHI, M. SASAKI, *Int. J. Radiat. Biol.* **1992**, *61*, 785–790.

[24] J.-C. Poully, J. Miles, S. De Camillis, A. Cassimi, J. B. Greenwood, *Phys. Chem. Chem. Phys.* **2015**, *17*, 7172–7180.

[25] B. L. Henke, E. M. Gullikson, J. C. Davis, *At. Data Nucl. Data Tables* **1993**, *54*, 181–342.

[26] W. Li, O. Kavatsyuk, W. Douma, X. Wang, R. Hoekstra, D. Mayer, M. S. Robinson, M. Gühr, M. Lalande, M. Abdelmouleh, M. Ryszka, J. C. Poully, T. Schlathölter, *Chem. Sci.* **2021**, DOI 10.1039/D1SC02885E.

[27] J. Czapla-Masztafiak, J. Szlachetko, C. J. Milne, E. Lipiec, J. Sá, T. J. Penfold, T. Huthwelker, C. Borca, R. Abela, W. M. Kwiatek, *Biophys. J.* **2016**, *110*, 1304–1311.

[28] D. Egorov, R. Hoekstra, T. Schlathölter, *Phys. Chem. Chem. Phys.* **2017**, *19*, 20608–20618.

[29] D. Egorov, L. Schwob, M. Lalande, R. Hoekstra, T. Schlatholter, *Phys. Chem. Chem. Phys.* **2016**, *18*, 26213–26223.

[30] M. Lalande, M. Abdelmouleh, M. Ryszka, V. Vizcaino, J. Rangama, A. Mery, F. Durantel, T. Schlatholter, J.-C. Poully, *Phys. Rev. A* **2018**, *98*, 062701.

[31] R. Franke, J. Hormes, *Phys. B Condens. Matter* **1995**, *216*, 85–95.

[32] J. Ni, M. A. A. Mathews, J. A. McCloskey, *Rapid Commun. Mass Spectrom.* **1997**, *11*, 535–540.

[33] A. Favre, F. Gonnet, J. Tabet, *Eur. J. MASS Spectrom.* **2000**, *6*, 389–396.

[34] C. S. Hoaglund, Y. S. Liu, A. D. Ellington, M. Pagel, D. E. Clemmer, *J. Am. Chem. Soc.* **1997**, *119*, 9051–9052.

[35] E. Itälä, M. A. Huels, E. Rachlew, K. Kooser, T. Hagerth, E. Kukk, *J. Phys. B-At. Mol. Opt. Phys.* **2013**, *46*.

[36] J. Kruse, P. Leinweber, K.-U. Eckhardt, F. Godlinski, Y. Hu, L. Zuin, *J. Synchrotron Radiat.* **2009**, *16*, 247–259.

[37] J. J. Neville, A. Jürgensen, R. G. Cavell, N. Kosugi, A. P. Hitchcock, *Chem. Phys.* **1998**, *238*, 201–220.

[38] *NIST Chemistry WebBook, NIST Standard Reference Database Number 69*, P.J. Linstrom And W.G. Mallard, **n.d.**

[39] M. Abdelmouleh, M. Lalande, V. Vizcaino, T. Schlatholter, J.-C. Poully, *Chem.- Eur. J.* **2020**, *26*, 2243–2250.

[40] J. Bockova, A. Rebelo, M. Ryszka, R. Pandey, T. da Fonseca Cunha, P. Limao-Viena, N. J. Mason, J. C. Poully, S. Eden, *Int. J. Mass Spectrom.* **2019**, *442*, 95–101.

[41] S. Maclot, D. Grzegorz Piekarski, A. Domaracka, A. Mery, V. Vizcaino, L. Adoui, F. Martin, M. Alcami, B. A. Huber, P. Rousseau, S. Diaz-Tendero, *J. Phys. Chem. Lett.* **2013**, *4*, 3903–3909.

[42] S. Ling, M. Gutowski, *J. Phys. Chem. A* **2016**, *120*, 8199–8210.

[43] R. N. Sodhi, R. G. Cavell, *J. Electron Spectrosc. Relat. Phenom.* **1983**, *32*, 283–312.

[44] L. Schwob, M. Lalande, J. Rangama, D. Egorov, R. Hoekstra, R. Pandey, S. Eden, T. Schlatholter, V. Vizcaino, J.-C. Poully, *Phys. Chem. Chem. Phys.* **2017**, *19*, 18321–18329.

[45] P. Zhou, K. Han, *Acc. Chem. Res.* **2018**, *51*, 1681–1690.

[46] L. Zhao, G. Zhou, B. Jia, G. Teng, K. Zhan, H. Zheng, J. Luo, B. Liu, *J. Photochem. Photobiol. Chem.* **2020**, *401*, 112753.

[47] E. P. Mansson, S. De Camillis, M. C. Castrovilli, M. Galli, M. Nisoli, F. Calegari, J. B. Greenwood, *Phys. Chem. Chem. Phys.* **2017**, *19*, 19815–19821.

[48] A. Golan, K. B. Bravaya, R. Kudirka, O. Kostko, S. R. Leone, A. I. Krylov, M. Ahmed, *Nat. Chem.* **2012**, *4*, 323–329.

[49] J.-C. Poully, V. Vizcaino, L. Schwob, R. Delaunay, J. Kocisek, S. Eden, J.-Y. Chesnel, A. Mery, J. Rangama, L. Adoui, B. Huber, *Chemphyschem* **2015**, *16*, 2389–2396.

[50] J.-Y. Wu, P.-Y. Cheng, *J. Phys. Chem. A* **2019**, *123*, 10700–10713.

[51] L. Tiefenthaler, S. Kollotzek, A. M. Ellis, P. Scheier, O. Echt, *Phys. Chem. Chem. Phys.* **2020**, *22*, 28165–28172.

[52] C.-C. Shen, T.-T. Tsai, J.-Y. Wu, J.-W. Ho, Y.-W. Chen, P.-Y. Cheng, *J. Chem. Phys.* **2017**, *147*, 164302.

[53] R. H. Duncan Lyngdoh, H. F. Schaefer, *Acc. Chem. Res.* **2015**, *42*, 563.

[54] A. Kumar, M. D. Sevilla, *J. Phys. Chem. B* **2009**, *113*, 11359–11361.

[55] N. J. Kim, H. M. Kim, S. K. Kim, *Int. J. Mass Spectrom.* **2007**, *261*, 32–37.

[56] S. Bari, O. Gonzalez-Magana, G. Reitsma, J. Werner, S. Schippers, R. Hoekstra, T. Schlatholter, *J. Chem. Phys.* **2011**, *134*, 024314.

[57] J. Viefhaus, F. Scholz, S. Deinert, L. Glaser, M. Ilchen, J. Seltmann, P. Walter, F. Siewert, *Nucl. Instrum. Methods Phys. Res. Sect. -Accel. Spectrometers Detect. Assoc. Equip.* **2013**, *710*, 151–154.

[58] R. E. LaVilla, *J. Chem. Phys.* **1972**, *57*, 899–909.

[59] M. Kato, Y. Morishita, M. Oura, H. Yamaoka, Y. Tamenori, K. Okada, T. Matsudo, T. Gejo, I. H. Suzuki, N. Saito, *J. Electron Spectrosc. Relat. Phenom.* **2007**, *160*, 39–48.

[60] K. Hirsch, J. T. Lau, P. Klar, A. Langenberg, J. Probst, J. Rittmann, M. Vogel, V. Zamudio-Bayer, T. Möller, B. von Issendorff, *J. Phys. B At. Mol. Opt. Phys.* **2009**, *42*, 154029.

MANUSCRIPT

WILEY-VCH